inorganics

MDPI

Article

A Rapid and Low-Cost Synthesis of ZSM-5 Single Crystals: The Inhibitory Effect of NH_4F on Twinning

Juan Du [1], Xiang Wan [2,3,*], Caixiong Song [4,5,*], Kangsheng Wu [4,5], Wenbing Yang [4,5], Beiye Liu [4,5], Qi Yang [4,5], Jingjing Fang [6] and Ayesha Razzaq [7]

1 College of Natural Resources and Geographic Information, Hubei Land Resources Vocational College, Wuhan 430090, China; juandu@alumni.ait.asia
2 Laboratory of Soil Health and Green Remediation, College of Resources and Environment, Huazhong Agricultural University, Wuhan 430070, China
3 Hubei Geological Survey, Wuhan 430034, China
4 Eighth Geological Brigade of Hubei Geological Bureau, Xiangyang 441000, China; wxb1662251105@163.com (K.W.); ywb-88@163.com (W.Y.); 13986366961@163.com (B.L.); yangqiyangqi2024@163.com (Q.Y.)
5 Hubei Key Laboratory of Resource and Eco-Environment Geology, Hubei Geological Bureau, Wuhan 430034, China
6 College of Environment and Engineering, Hubei Land Resources Vocational College, Wuhan 430090, China; fangjingjing0720@163.com
7 Key Laboratory of Engineering Plastics, Beijing National Laboratory for Molecular Science, Institute of Chemistry, Chinese Academy of Sciences, Beijing 100190, China; aishrazz@gmail.com
* Correspondence: wxzgdz@webmail.hzau.edu.cn (X.W.); m757062526@163.com (C.S.)

Abstract

Crystal twinning, a common growth phenomenon, can substantially affect material performance in fields such as semiconductors, nonlinear optics, and drug development, yet its elimination during crystallization is challenging. This study presents a method for the controlled synthesis of ZSM-5 zeolite as either single crystals or twinned crystals using kaolin as the primary raw material. The method leverages the etching effect of ammonium fluoride (NH_4F) on the aluminosilicate structure derived from pre-treated kaolin. By adjusting the concentrations of NH_4F and the structure-directing agent tetrapropylammonium bromide (TPABr), pure ZSM-5 single crystals and twinned crystals were selectively synthesized. Conventionally, NH_4F is employed to introduce defects into zeolite structures. In contrast, this work demonstrates its utility in controlling crystal habit. The synthesis utilizes kaolin, an abundant and low-cost aluminosilicate mineral, to provide the entire aluminum source and a portion of the silicon source, offering an economical alternative to expensive precursors like aluminum isopropoxide. The resulting single and twinned crystals exhibited high crystallinity, demonstrating the viability of using natural minerals to produce high-quality zeolites. The physical and chemical properties of the kaolin-derived ZSM-5 were characterized and compared to those of ZSM-5 synthesized from conventional chemical reagents. A growth mechanism for the formation of single and twinned crystals is also proposed.

Keywords: kaolin; single crystal; ZSM-5; aluminum; twinning control

check for updates

Academic Editor: Richard Dronskowski

Received: 8 July 2025
Revised: 6 August 2025
Accepted: 13 August 2025
Published: 18 August 2025

Citation: Du, J.; Wan, X.; Song, C.; Wu, K.; Yang, W.; Liu, B.; Yang, Q.; Fang, J.; Razzaq, A. A Rapid and Low-Cost Synthesis of ZSM-5 Single Crystals: The Inhibitory Effect of NH_4F on Twinning. *Inorganics* **2025**, *13*, 272. https://doi.org/10.3390/inorganics13080272

Copyright: © 2025 by the authors. Licensee MDPI, Basel, Switzerland. This article is an open access article distributed under the terms and conditions of the Creative Commons Attribution (CC BY) license (https://creativecommons.org/licenses/by/4.0/).

1. Introduction

Crystal twinning can substantially affect material performance in fields such as semiconductors [1], nonlinear optics [2], and drug development [3], making its control a significant scientific challenge. Zeolites are a class of aluminosilicates characterized by a

three-dimensional framework structure with uniform micropores. Their well-defined pore architecture, combined with high catalytic activity and thermal stability, has led to their extensive application in catalysis, adsorption, and ion exchange [4,5]. Among them, ZSM-5 zeolite exhibits excellent catalytic performance and is widely used in petrochemical processes such as catalytic cracking [6], isomerization [7], aromatization [8], and alkylation [9].

As an abundant mineral resource composed primarily of aluminosilicates, kaolin is an attractive and low-cost precursor for the synthesis of various zeolites [10–13], offering an alternative to more expensive reagents like aluminum isopropoxide [14]. Previous studies have reported the synthesis of ZSM-5 from kaolin and illite [15,16]; however, issues such as low sample purity, poor crystallinity, and the absence of a well-defined structure have limited the practical application of these mineral-based routes. A significant obstacle is the high structural stability of kaolin, which necessitates an activation pretreatment before it can be used as a reactive raw material.

This study employed a low-cost alkaline thermal activation treatment to convert kaolin into acid-soluble sodalite [17]. Subsequent adjustment of the pH of the acid hydrolysis solution yielded an amorphous silica-alumina gel. A challenge with such gels is that their three-dimensional network structure prevents the raw materials from participating in the crystallization reaction as uniformly as pure chemical reagents, thereby limiting the quality of the final product. To address this, we utilized the known etching effect of the fluoride ion (F^-) on aluminosilicate structures [18,19]. While fluoride sources have previously been used to assist in the dissolution of silica-alumina gels [20,21], their role has generally been limited to pretreatment or non-selective etching. To the best of our knowledge, this is the first report on the strategic use of NH_4F concentration to selectively control the formation of either single or twinned ZSM-5 crystals derived from a mineral precursor. In our approach, ammonium fluoride (NH_4F) was introduced as a "structural shearing agent" to break down the gel network, allowing the silica and alumina species to be more evenly dispersed in the reaction mixture.

By systematically adjusting the concentration of NH_4F, we achieved the controlled synthesis of ZSM-5 with high crystallinity in the form of either single crystals or twinned crystals. This advancement facilitates the use of processed minerals as a substitute for pure chemical reagents in zeolite synthesis. The as-synthesized samples were ion-exchanged to produce the protonated form (H-ZSM-5). For comparison, a ZSM-5 sample was also synthesized using aluminum isopropoxide as the aluminum source. The materials were characterized using X-ray diffraction (XRD), scanning electron microscopy (SEM), energy-dispersive X-ray spectroscopy (EDS), Fourier-transform infrared spectroscopy (FT-IR), N_2 adsorption-desorption, and ammonia temperature-programmed desorption (NH_3-TPD). Finally, a formation mechanism for the single and twinned crystals is discussed.

2. Results and Discussion

2.1. X-Ray Diffraction Analysis

The phase purity and crystallinity of the synthesized materials were examined by XRD. Figure 1 displays the XRD patterns of the samples. A-HZSM-5 and K-HZSM-5 denote H-ZSM-5 zeolites synthesized with aluminum isopropoxide and kaolin-derived silica-alumina gel as the aluminum source, respectively. The numbers in parentheses indicate the molar ratio of NH_4F in the synthesis gel. The black vertical lines represent the standard diffraction pattern for ZSM-5 (PDF#42-0024).

All samples, except for A-HZSM-5 (0.05 M), exhibit the characteristic diffraction peaks of the MFI framework structure, confirming the formation of ZSM-5 zeolite. A comparison of the patterns reveals that the addition of NH_4F did not inhibit the formation of the ZSM-5 structure when the silica-alumina gel was used. In contrast, when aluminum

isopropoxide was the aluminum source, the presence of NH_4F resulted in an amorphous product. A crystalline ZSM-5 phase was only obtained from aluminum isopropoxide in the absence of NH_4F. This suggests that without the buffering effect of the silica-alumina gel, NH_4F disrupts the crystallization of ZSM-5.

The XRD patterns of the raw kaolin, the activated sodalite, and the final silica-alumina gel are shown in the Appendix A (Figure A1). The pattern of the raw material corresponds well with the standard for kaolin (PDF#78-1996), with minor impurities of quartz and mica. After alkaline thermal activation, these components were converted into a pure sodalite phase (PDF#76-1639). Subsequent acid dissolution and washing yielded an amorphous silica-alumina gel, as confirmed by the absence of sharp diffraction peaks.

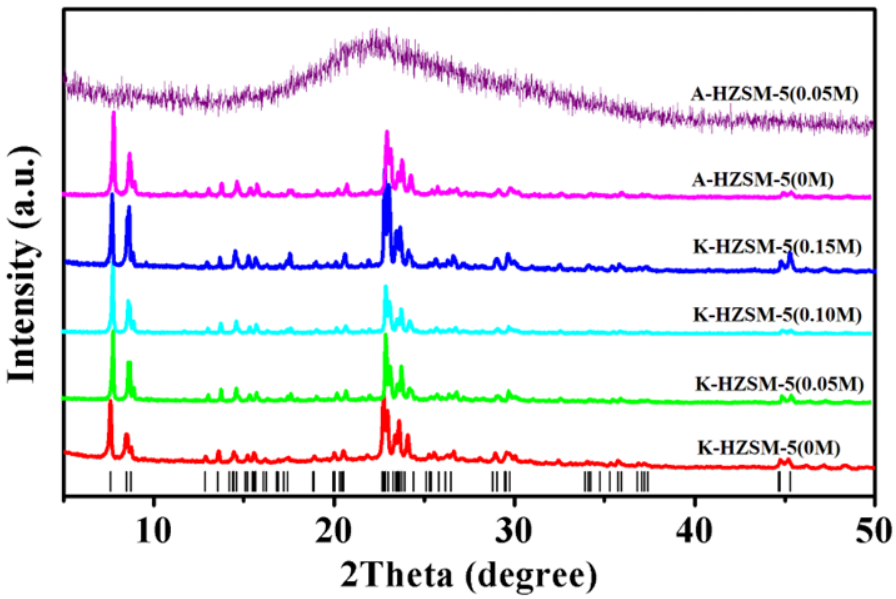


Figure 1. XRD patterns of samples prepared with different aluminum sources and NH_4F concentrations.

2.2. Surface Morphology and Elemental Analysis

The morphology of the synthesized ZSM-5 samples was investigated by SEM. As shown in Figure 2a, when the silica-alumina gel was used as the raw material without NH_4F, the resulting product consisted of irregularly shaped and sized elliptical particles, with a noticeable amount of unreacted amorphous material. This suggests that the three-dimensional network within the gel hinders its uniform dispersion and participation in the reaction.

Upon the addition of 0.10 M NH_4F (Figure 2c), uniformly dispersed, well-defined twinned crystals of ZSM-5 were obtained, with almost no residual amorphous phase. This indicates that F^- acts as a shearing agent, effectively breaking down the gel's network structure into smaller, more reactive molecular species that can participate uniformly in the crystallization process. When the NH_4F concentration was increased to 0.15 M (Figure 2b), the product was composed of pure single crystals of ZSM-5.

Further adjustments to the NH_4F concentration affected the crystal morphology (Figure A2). An insufficient amount of NH_4F (0.05 M) did not significantly improve the crystallization. Conversely, an excessive amount (0.20 M) led to the formation of many crystals with incomplete or etched structures, likely due to the strong etching effect of F^- on the ZSM-5 framework.

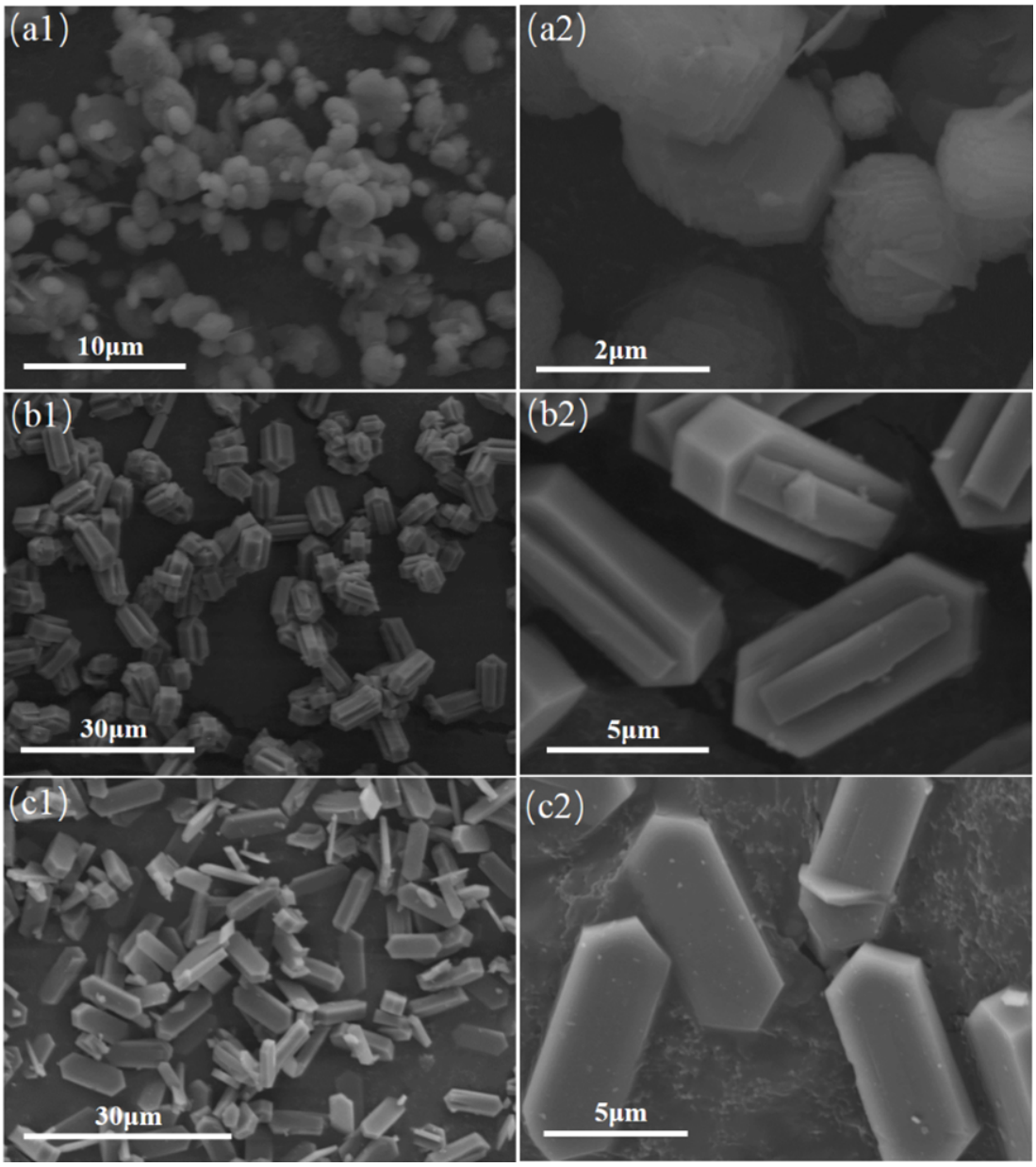


Figure 2. SEM images of (**a1**,**a2**) K-HZSM-5 (0 M), (**b1**,**b2**) K-HZSM-5 (0.15 M), and (**c1**,**c2**) K-HZSM-5 (0.10 M).

EDS analysis was performed on the synthesized single crystal and twinned crystal ZSM-5 (Figures 3 and 4). The EDS maps confirm the homogeneous distribution of silicon (Si), oxygen (O), and aluminum (Al) throughout the crystals, which is critical for uniform acid site distribution. The absence of sodium (Na) indicates that the ion-exchange process was complete. The elemental composition, showing a high proportion of Si and O with a smaller amount of Al, is consistent with that of high-silica ZSM-5 zeolite.

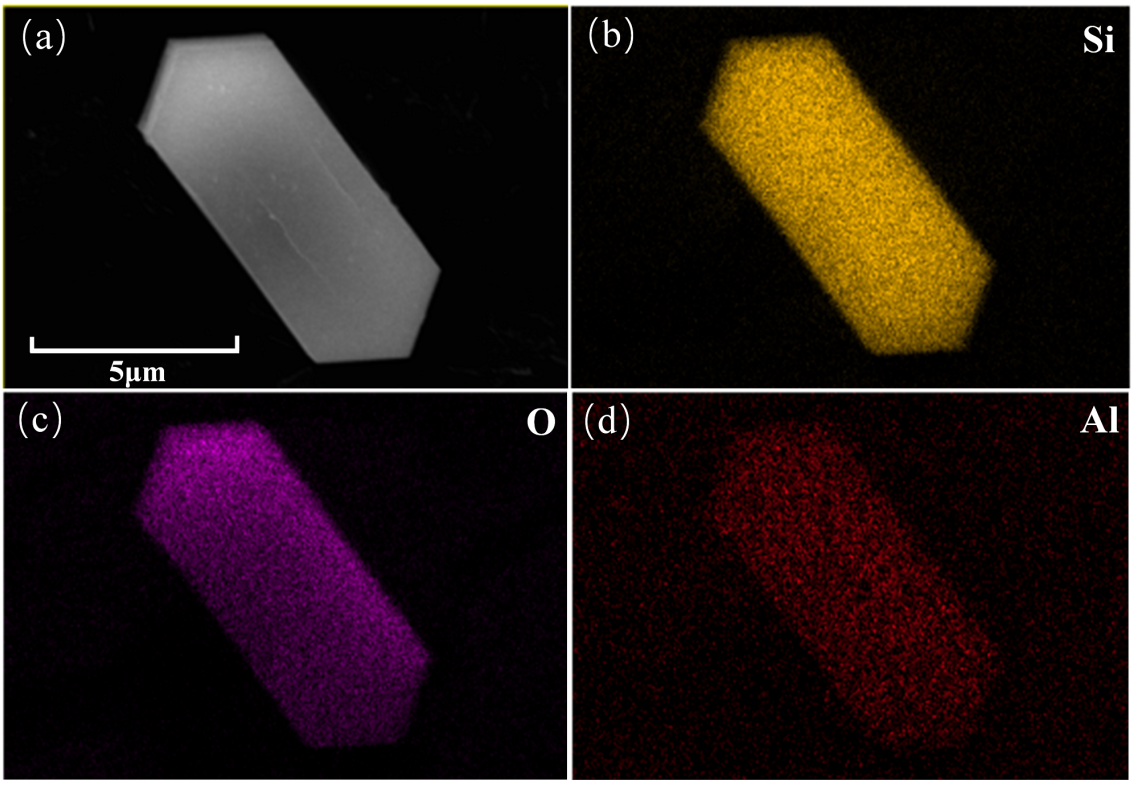


Figure 3. EDS analysis of a single crystal ZSM-5 sample (K-HZSM-5 (0.15 M)): (**a**) SEM image of the selected crystal; and corresponding elemental maps for (**b**) Silicon (Si), (**c**) Oxygen (O), and (**d**) Aluminum (Al), demonstrating the uniform distribution of elements.

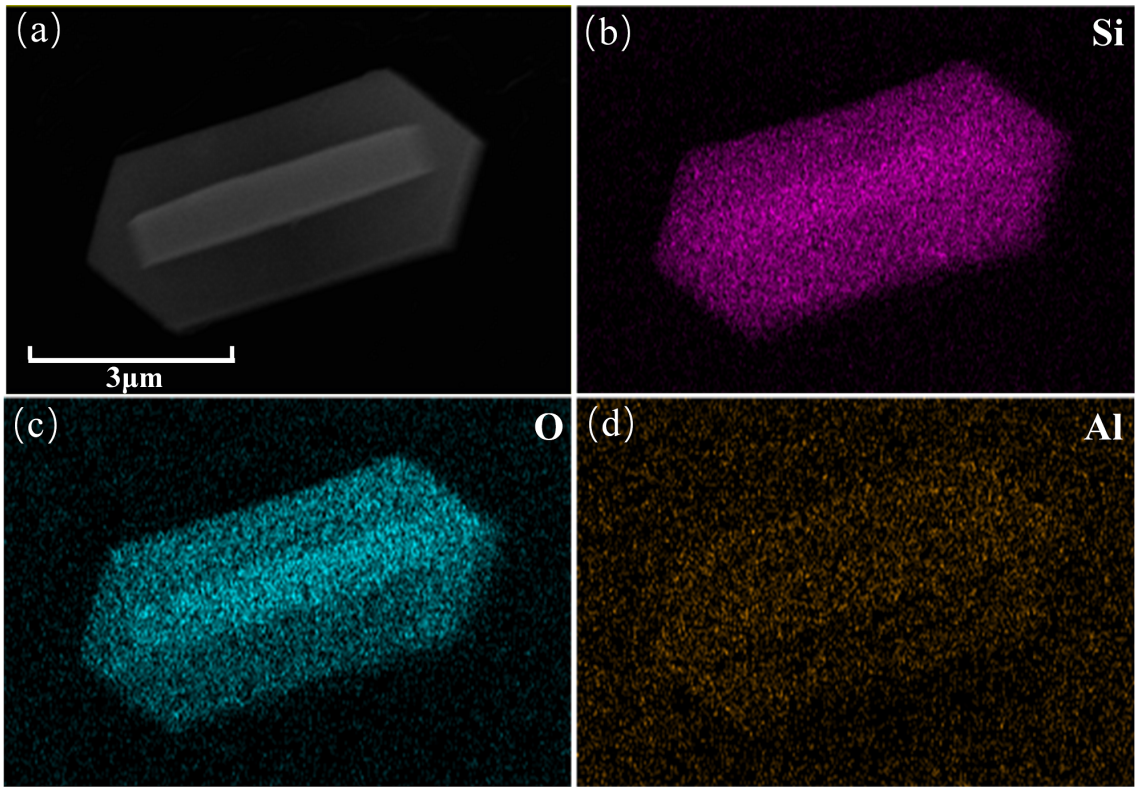


Figure 4. EDS analysis of a single crystal ZSM-5 sample (K-HZSM-5 (0.10 M)): (**a**) SEM image of the selected crystal; and corresponding elemental maps for (**b**) Silicon (Si), (**c**) Oxygen (O), and (**d**) Aluminum (Al).

2.3. FT-IR Spectrum Analysis

FT-IR spectroscopy was used to analyze the structural transformations of kaolin and the final zeolite products. The spectra of the raw kaolin, sodalite, and silica-alumina gel are provided in the Appendix A (Figure A3). The absorption peaks for kaolin and sodalite are consistent with those reported in the literature [22–25]. The spectrum of the silica-alumina gel, the direct precursor for ZSM-5 synthesis, shows a broad band at 1005 cm^{-1} due to Si-O stretching vibrations, bands at 707 and 574 cm^{-1} representing Si-O-Al bending vibrations, and a band at 445 cm^{-1} associated with internal T-O (T = Si, Al) bending vibrations [26,27].

Figure 5 presents the FT-IR spectra of the final calcined samples in the 1500–400 cm^{-1} region. All samples display absorption bands at approximately 1225, 1080, 790, 550, and 440 cm^{-1}, which are characteristic of the ZSM-5 framework structure [28]. This confirms that the single crystals and twinned crystals synthesized from silica-alumina gel, as well as the ZSM-5 synthesized from aluminum isopropoxide, all possess the correct MFI topology. Specifically, the band at 440 cm^{-1} corresponds to T-O bending vibrations [29]. The band at 550 cm^{-1} is attributed to the vibration of the double five-membered ring units that are characteristic of the ZSM-5 structure [30]. The bands at 790 cm^{-1} and 1080 cm^{-1} are assigned to symmetric and internal asymmetric stretching vibrations of T-O-T linkages, respectively [31]. The band at 1225 cm^{-1} is due to external asymmetric stretching of T-O-T linkages [32].

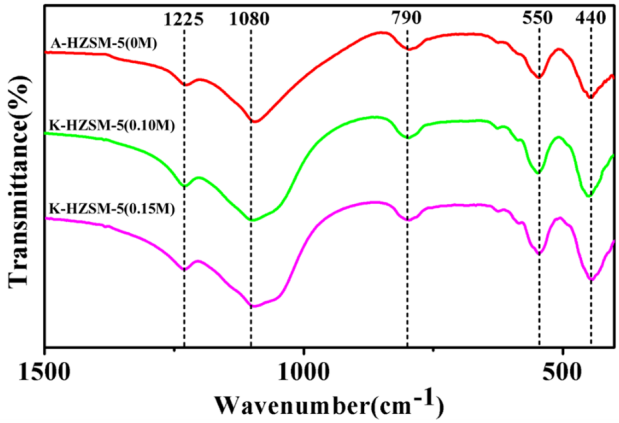


Figure 5. FT−IR spectra of the as-synthesized ZSM-5 samples.

2.4. N_2 Adsorption-Desorption Analysis

The textural properties of the samples were evaluated by N_2 physisorption. The adsorption-desorption isotherms and corresponding pore size distributions are shown in Figures 6 and 7, respectively. The key textural parameters are summarized in Table 1. The specific surface areas of all synthesized samples are higher than that of a commercial ZSM-5 (309 m^2/g) reported previously [33].

The isotherm for the single crystal sample, K-HZSM-5 (0.15 M), is a type I isotherm, which is characteristic of microporous materials and typical for conventional ZSM-5 [34]. In contrast, the twinned crystal sample, K-HZSM-5 (0.10 M), and the sample synthesized from aluminum isopropoxide, A-HZSM-5 (0 M), both exhibit type IV isotherms with hysteresis loops, indicating the presence of mesoporosity. The hysteresis is slight for the twinned crystal sample but more pronounced for the A-HZSM-5 (0 M) sample, suggesting a larger volume of mesopores in the latter.

The pore volume and specific surface area are important factors influencing a zeolite's performance. As shown in Table 1, the textural properties of the single and twinned crystal ZSM-5 synthesized from kaolin are comparable or superior to those of the sample made from pure chemical reagents, affirming the viability of the mineral-based synthesis route.

A comparison between the two kaolin-derived samples shows that the single crystal has a slightly higher specific surface area, while the presence of some mesoporosity in the twinned crystal may be advantageous for certain catalytic applications by facilitating mass transport. The BJH pore size distribution (Figure 7) confirms that all samples have a primary pore size distribution centered below 2 nm, consistent with the micropores of ZSM-5.

Table 1. Textural properties of the ZSM-5 samples.

Sample	S_{BET} [a] (m^2g^{-1})	S_{micro} [c] (m^2g^{-1})	S_{meso} [b] (m^2g^{-1})	V_{total} [d] (cm^3g^{-1})	V_{micro} [f] (cm^3g^{-1})	V_{meso} [e] (cm^3g^{-1})
A-HZSM-5 (0 M)	322	198	123	0.16	0.12	0.04
K-HZSM-5 (0.10 M)	351	280	71	0.18	0.15	0.03
K-HZSM-5 (0.15 M)	385	316	69	0.19	0.16	0.03

[a] BET surface area. [b] $S_{Meso} = S_{BET} - S_{Micro}$. [c] t-plot micropore surface area. [d] Pore volume at $p/p_0 = 0.99$. [e] $V_{Meso} = V_{Total} - V_{Micro}$. [f] t-plot micropore volume.

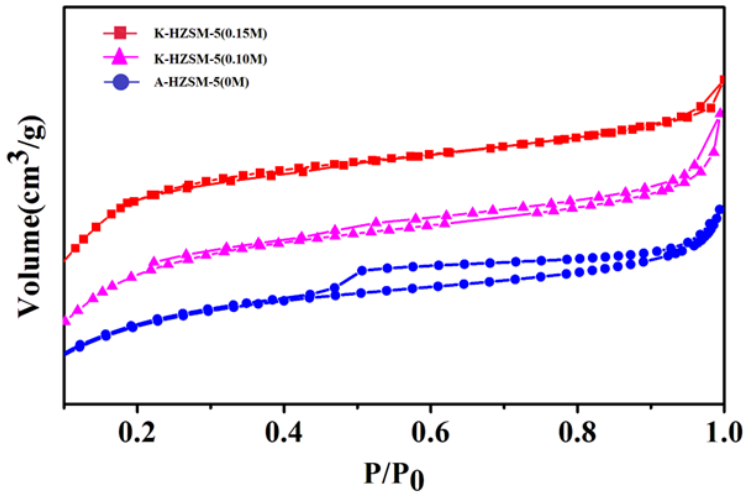


Figure 6. N_2 adsorption-desorption isotherms of ZSM-5 samples.

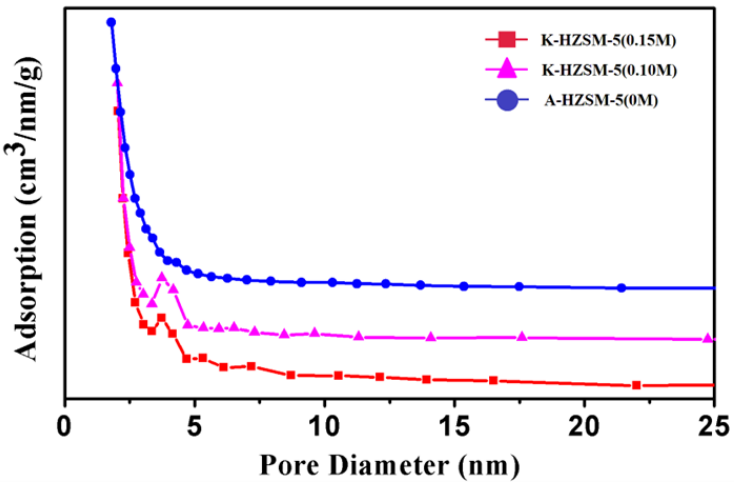


Figure 7. BJH pore-size distributions of samples.

2.5. Evaluation of Surface Acidity

The acid properties of the protonated H-ZSM-5 zeolites were investigated using NH_3-TPD analysis. The profiles in Figure 8 show two distinct NH_3 desorption peaks for each sample. The low-temperature (LT) peak, between 100–300 °C, is assigned to NH_3 desorbing from weak acid sites, while the high-temperature (HT) peak, between

300–500 °C, corresponds to desorption from strong acid sites [35]. The quantified acid site densities are listed in Table 2.

The NH_3-TPD profiles of the single crystal K-HZSM-5(0.15M) and the twinned crystal K-HZSM-5(0.10M) are very similar. In ZSM-5, strong Brønsted acidity originates from tetrahedrally coordinated aluminum within the framework, whereas weaker acidity is typically associated with surface silanol (Si-OH) groups or extra-framework aluminum species [36,37]. The similarity in the profiles indicates that the single and twinned crystals possess comparable internal structures and distributions of framework aluminum. The sample synthesized from aluminum isopropoxide exhibits a higher total acidity, but a lower concentration of strong acid sites, which may affect its catalytic performance in reactions requiring strong acid catalysis. The kaolin-derived single and twinned crystals, with their substantial fraction of strong acid sites, may be more suitable for such applications.

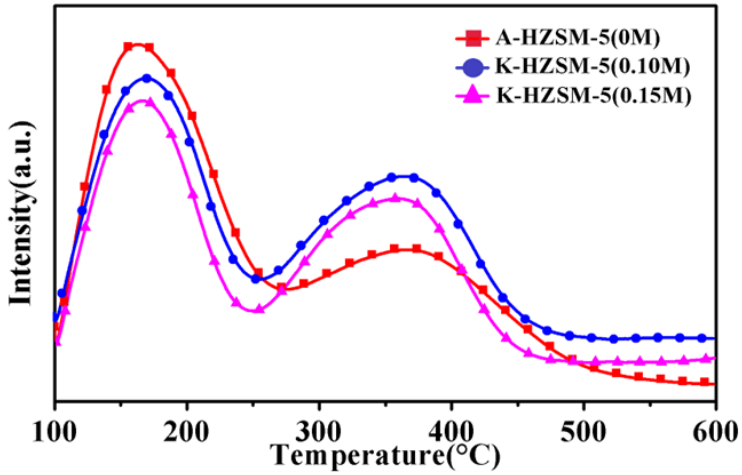


Figure 8. NH_3-TPD profiles of ZSM-5 samples.

Table 2. Acid properties of ZSM-5 samples.

Sample	Weak Acidity (mmol g^{-1})	Strong Acidity (mmol g^{-1})	Total Acidity (mmol g^{-1})
A-HZSM-5 (0 M)	5.91	1.25	7.16
K-HZSM-5 (0.10 M)	3.50	2.44	5.94
K-HZSM-5 (0.15 M)	3.59	2.53	6.12

2.6. Discussion on the Formation Mechanism

Figure 9 provides a schematic illustration of the ZSM-5 crystal structure. ZSM-5 crystallizes in the orthorhombic system with unit cell parameters of a ≈ 20.1 Å, b ≈ 19.9 Å, and c ≈ 13.4 Å [38]. Because the lengths of the a- and b-axes are very similar, twinning frequently occurs across the (010) plane, resulting in the characteristic intergrown structure shown on the right side of Figure 9.

The growth process can be understood in the context of the Kossel-Stranski model of layer growth [39]. As illustrated in Figure 10(1), crystal growth preferentially occurs at sites with the highest coordination, such as kink sites a ≈ 20.1 Å, b ≈ 19.9 Å, and c ≈ 13.4 Å [38]. (three-sided concave corners, position a) and step sites (two-sided concave corners, position b), rather than on flat terraces (general position c). For crystals like ZSM-5 where the a- and b-axes are similar, twinning can relieve internal strain and enhance stability. The formation of a twin boundary creates a permanent re-entrant (concave) corner, as shown in Figure 10(2), which acts as a continuous source of new step sites,

promoting rapid growth in that direction. Consequently, in conventional synthesis systems, the formation of twinned crystals is often favored and difficult to suppress.

In this study, we propose that the presence of F^- ions at an appropriate concentration inhibits the formation of these twin boundaries. The F^- ions are known to etch aluminosilicate structures. We hypothesize that this etching effect preferentially removes or passivates the nucleation sites on the (010) crystal face that would otherwise lead to twinning. This "shearing" action results in a smoother (010) plane, as depicted in Figure 10(3), which disfavors the intergrowth of a second crystal and thereby promotes the formation of single crystals.

It is known that NH_4F can introduce mesoporosity and framework defects in ZSM-5, as demonstrated by Bolshakov et al. [18]. However, the N_2 physisorption data for our single-crystal sample (K-HZSM-5 (0.15 M)) shows a Type I isotherm with minimal hysteresis, suggesting that under our specific synthesis conditions, particularly the presence of the reactive silica-alumina gel and a controlled NH_4F concentration, the dominant role of fluoride is the moderation of crystal growth rather than aggressive framework etching. We speculate that NH_4F primarily acts during the crystal growth stage, after nucleation. Its function is likely to selectively passivate or etch the (010) crystal face, which is prone to twinning, thereby inhibiting intergrowth and promoting the development of single crystals. Further kinetic studies would be required to definitively confirm this proposed mechanism.

The presence of twin boundaries in ZSM-5 crystals can disrupt the continuity of the straight micropore channels. This disruption creates longer, more tortuous diffusion pathways for reactant and product molecules, which can lead to increased diffusion limitations and potentially lower catalytic activity or faster deactivation. The synthesis of single crystals, as demonstrated in our work, mitigates this structural issue by providing unobstructed transport pathways through the zeolite framework.

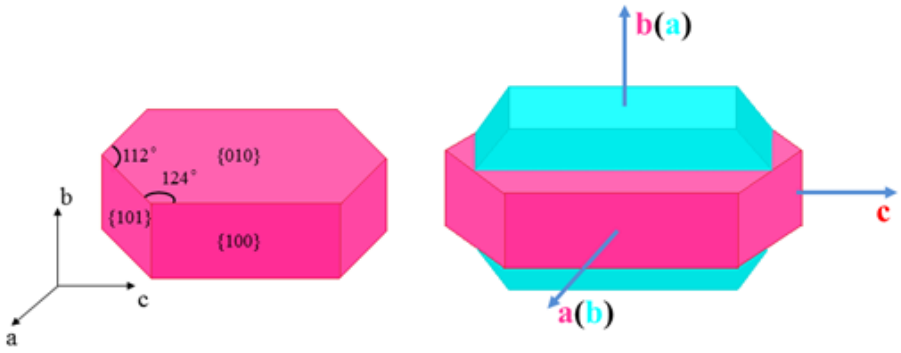


Figure 9. Schematic diagram of single and twinned ZSM-5 zeolite crystals.

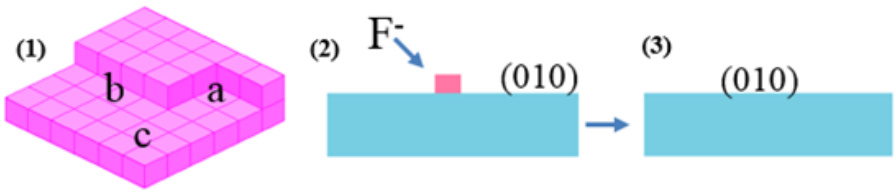


Figure 10. Proposed crystal growth mechanism illustrating the inhibition of twinning by F^-.

3. Materials and Methods

3.1. Materials

Kaolin minerals and natural quartz (SiO_2, 99 wt%) were supplied by Xinyisheng Advanced Technology Co., Ltd., Xiamen, China. The chemical reagents included sodium hydroxide (NaOH, 96 wt%) and ammonium chloride (NH_4Cl, 99.5 wt%), which were purchased from Sinopharm Chemical Reagent Co., Ltd., Shanghai, China. Sulfuric acid (H_2SO_4,

98 wt%) and ammonium fluoride (NH_4F, 96 wt%) were purchased from Xilong Chemical Co., Ltd., Chengdu, China. Tetrapropylammonium bromide (TPABr, $(CH_3CH_2CH_2)_4N(Br)$, 98 wt%) was acquired from Aladdin Industrial Co., Ltd., Shanghai, China. Fumed silica (SiO_2, 99.8 wt%) was sourced from Evonik Degussa, Xiamen, China. All chemical reagents were used as received without further purification.

3.2. Pre-Treatment of Minerals

To prepare the sodium silicate solution, quartz (3.60 g, 0.06 mol) and NaOH (4.80 g, 0.12 mol) were combined with 50 mL of deionized water in a beaker. The mixture was transferred to a 100 mL polytetrafluoroethylene-lined stainless steel autoclave and heated at 463 K for 24 h. The resulting product was centrifuged, washed three times with deionized water, and dried at 343 K for 24 h to obtain sodium silicate powder.

The pretreatment of kaolin involved three steps. First, the as-received kaolin was activated. Kaolin (0.5 g) was mixed with 10 mL of 6 M NaOH solution in a 25 mL polytetrafluoroethylene-lined stainless steel autoclave and reacted at 473 K for 5 h to produce sodalite. Second, the sodalite was dissolved by adding 5 mL of 1 M H_2SO_4 solution and stirring. Third, the pH of the resulting clear solution was adjusted to 7.0 with NaOH solution to precipitate a white gel. This silica-alumina gel was collected by filtration, washed, and used in subsequent syntheses.

3.3. Synthesis of ZSM-5

ZSM-5 zeolite was synthesized via a conventional hydrothermal method. A mixture of sodium silicate, silica-alumina gel, TPABr, and deionized water was prepared at room temperature with thorough stirring. Fumed silica was then rapidly added to the solution. The final molar composition of the synthesis gel was SiO_2: 0.02 Al_2O_3: 0.16 Na_2O: 0.2 TPABr: x NH_4F: 185 H_2O, where x was varied (0, 0.05, 0.10, 0.15, and 0.20). The homogeneous gel was transferred to a polytetrafluoroethylene-lined stainless steel autoclave and heated at 473 K for 48 h.

After the reaction, the samples were collected by centrifugation, washed three times with deionized water, and dried. To obtain the protonated form, ion exchange was performed by treating the samples with a 1 M NH_4Cl solution at 343 K for 6 h. This process was repeated three times. Finally, the samples were calcined at 823 K for 5 h to remove the organic template, yielding H-ZSM-5 zeolite. A comparative sample (A-HZSM-5) was synthesized under identical conditions, but using aluminum isopropoxide as the aluminum source. Samples derived from kaolin are denoted as K-HZSM-5.

3.4. Characterization

Powder X-ray diffraction (XRD) patterns were collected on a Bruker-D8 diffractometer with Cu Kα radiation (40 kV, 40 mA) over a 2θ range of 5–50°. The surface morphology of the samples was examined using a SU-70 field-emission scanning electron microscope (SEM) at an accelerating voltage of 10 kV. Elemental analysis was conducted using an energy-dispersive X-ray spectrometer (EDS) attached to the SEM, operating at 20 kV. Fourier-transform infrared (FT-IR) spectra were recorded on a Nicolet iS10 spectrometer over a range of 4000–400 cm^{-1}.

Ammonia temperature-programmed desorption (NH_3-TPD) experiments were performed on a Micromeritics AutoChem II 2920 to determine the acid properties. Typically, 100 mg of catalyst was degassed in flowing helium at 600 °C for 1 h. After cooling to 100 °C, the sample was saturated with NH_3 for 30 min. Physisorbed ammonia was removed by purging with helium. The temperature was then ramped from 100 to 600 °C at a rate of 10 °C·min^{-1}, and the desorbed NH_3 was monitored.

Nitrogen adsorption-desorption isotherms were measured at 77 K using a Micromeritics ASAP 2460 system. Prior to the measurements, samples were outgassed under vacuum at 573 K for 6 h.

4. Conclusions

ZSM-5 zeolite, as either single crystals or twinned crystals, was successfully synthesized via a hydrothermal method using kaolin as the sole aluminum source and a partial silicon source. The introduction of F^- ions from NH_4F was effective in breaking down the network structure of the kaolin-derived silica-alumina gel, overcoming a common limitation in the use of mineral precursors for zeolite synthesis. By carefully adjusting the concentration of NH_4F, ZSM-5 zeolites with high crystallinity were selectively produced as either single crystals or twinned crystals. This work presents a simple and low-cost route for synthesizing high-quality zeolites from natural minerals as an alternative to pure chemical reagents.

Furthermore, this study demonstrates a different application for F^- in zeolite synthesis. While often used to create defects or modify structures, here it was employed to inhibit the growth of twinned crystals, enabling the formation of single crystals. Characterization by XRD, SEM, FT-IR, N_2 physisorption, and NH_3-TPD confirmed the successful synthesis and favorable properties of the kaolin-derived materials. A comparison of the single and twinned crystals revealed similar surface acidity, but the single crystals possessed a higher specific surface area. These findings suggest that by controlling the synthesis conditions, particularly the F^- concentration, it is possible to produce ZSM-5 single crystals with superior textural properties for various applications.

Author Contributions: Conceptualization, J.D.; formal analysis, J.D.; funding acquisition, J.D.; investigation, X.W., C.S. and B.L.; methodology, J.D. and W.Y.; software, J.D.; supervision, K.W. and Q.Y.; validation, J.D., X.W., A.R. and J.F.; visualization, J.D., X.W. and A.R.; writing—original draft, J.D. and C.S.; writing—review and editing, J.D. and A.R. All authors have read and agreed to the published version of the manuscript.

Funding: This research was funded by Central Environmental Protection Special Fund Project, Educational Science Planning Project of the Education Department of Hubei Province (grant no. 2024GB086); and Crossing Research Project of Hubei Land Resources Vocational College (grant no. HX2024ZX05, HX2024ZX12, HX2024ZX13, HX2025ZX09 and HX2025ZX11).

Institutional Review Board Statement: Not applicable.

Informed Consent Statement: Not applicable.

Data Availability Statement: The data presented in this study are available on request from the corresponding author.

Acknowledgments: The authors acknowledge the support of the shared scientific facilities at their respective institutions.

Conflicts of Interest: The authors declare no conflicts of interest.

Abbreviations

The following abbreviations are used in this manuscript:

XRD	X-ray Diffraction
SEM	Scanning Electron Microscopy
EDS	Energy Dispersive X-ray Spectroscopy
FT-IR	Fourier-Transform Infrared Spectroscopy
TPABr	Tetrapropylammonium bromide
NH_3-TPD	Ammonia Temperature-Programmed Desorption
LT	Low-Temperature
HT	High-Temperature

Appendix A

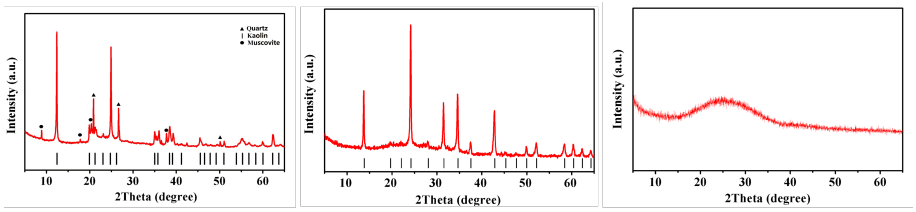


Figure A1. XRD patterns of (**a**) raw kaolin, (**b**) sodalite after activation, and (**c**) amorphous silica-alumina gel.

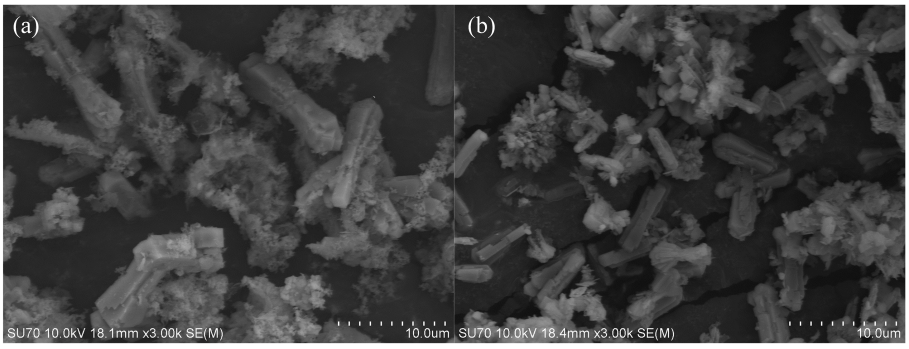


Figure A2. SEM images showing the effect of varying NH_4F concentration on ZSM-5 morphology: (**a**) 0.05 M and (**b**) 0.20 M.

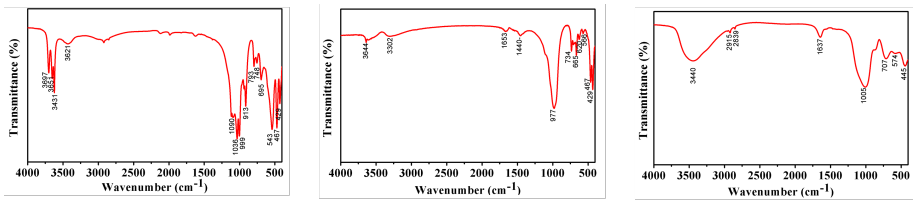


Figure A3. FT−IR spectra of (**a**) raw kaolin, (**b**) sodalite after activation, and (**c**) amorphous silica-alumina gel.

References

1. Chi, C.Y.; Chang, C.C.; Hu, S.; Yeh, T.W.; Cronin, S.B.; Dapkus, P.D. Strain Effects on Wurtzite/Zinc-Blende Biphase InAs Nanowires. *Nano Lett.* **2013**, *13*, 2506–2515. [CrossRef]
2. Babu, R.R.; Sethuraman, K.; Gopalakrishnan, R.; Ramasamy, P. Growth and characterization of L-arginine acetate single crystals. *J. Cryst. Growth* **2006**, *297*, 356–360.
3. Golzarroshan, B.; Siddegowda, M.S.; Li, H.Q.; Yathirajan, H.S.; Narayana, B.; Rathore, R.S. Crystal structure, Hirshfeld surface analysis and DFT studies of (E)-1-(4-chlorophenyl)-3-(4-nitrophenyl)prop-2-en-1-one. *J. Mol. Struct.* **2012**, *1018*, 107–112. [CrossRef]
4. Abate, S.; Barbera, K.; Centi, G.; Lanzafame, P.; Perathoner, S. Use of zeolites in the catalytic conversion of bio-ethanol to light olefins. *Catal. Sci. Technol.* **2016**, *6*, 2485–2501. [CrossRef]
5. de Pietre, M.K.; dos Santos, F.S.; de Almeida Ribeiro, J.A.; Neri, J.A.M.; de Oliveira, D.F. Removal of reactive dyes from aqueous solution by adsorption on natural zeolite. *Water Sci. Technol.* **2017**, *76*, 3441–3451.
6. Hou, X.; Qiu, Y.; Yuan, E.; Li, F.; Li, Z.; Ji, S.; Yang, Z.; Liu, G.; Zhang, X. Catalytic cracking of Jatropha oil for hydrocarbon liquid fuel over hierarchical ZSM-5 zeolite. *Appl. Catal. A Gen.* **2017**, *543*, 51–60. [CrossRef]
7. Rasouli, M.; Atashi, H.; Mohebbi-Kalhori, D.; Yaghobi, N. A kinetic study of n-hexane isomerization over Pt/HZSM-5 catalyst. *J. Taiwan Inst. Chem. Eng.* **2017**, *78*, 438–446. [CrossRef]
8. Fang, Y.; Tang, J.; Huang, X.; Shen, W.; Song, Y.; Sun, C. Aromatization of methanol over Zn-modified ZSM-5 zeolites. *Chin. J. Catal.* **2010**, *31*, 264–266. [CrossRef]

9. Hu, H.; Zhang, Q.; Cen, J.; Li, X. Alkylation of Benzene with Methanol over HZSM-5 Zeolites with Different Si/Al Ratios. *Catal. Lett.* **2015**, *145*, 715–722. [CrossRef]
10. Hartanto, D.; Kurniawati, R.; Pambudi, A.B.; Utomo, W.P.; Leaw, W.L.; Nur, H. The synthesis of ZSM-5 from kaolin without organic template. *Solid State Sci.* **2019**, *87*, 150–154. [CrossRef]
11. Hartati, H.; Widati, A.A.; Dewi, T.K.; Prasetyoko, D. Synthesis of ZSM-5 from Kaolin Clay using a Hydrothermal Method without an Organic Template. *Bull. Chem. React. Eng. Catal.* **2017**, *12*, 251. [CrossRef]
12. Holmes, S.M.; Khoo, S.H.; Kovo, A.S. The synthesis of zeolites from mineral sources. *Green Chem.* **2011**, *13*, 843–858.
13. Youssef, H.F.; Hegazy, W.H.; Abo-Almaged, H.H.; El-Bassyouni, G.T. Synthesis and Characterization of Zeolite A from Egyptian Kaolin. *Bioinorg. Chem. Appl.* **2015**, *2015*, 428121.
14. Liu, H.; Liu, G.; Zhang, X.; Zhao, D.; Wang, L. Synthesis of ZSM-5 zeolite with small crystal size from silica-alumina gel for catalytic cracking of n-heptane. *Microporous Mesoporous Mater.* **2017**, *244*, 164–170. [CrossRef]
15. Mohiuddin, E.; Isa, Y.M.; Mdleleni, M.M.; Sincadu, N.; Key, D.; Tshabalala, T. Synthesis of ZSM-5 from South African kaolin. *Appl. Clay Sci.* **2016**, *119*, 213–221. [CrossRef]
16. Liu, Y.; Han, S.; Guan, D.; Chen, S.; Wu, Y.; Yang, Y.; Jiang, N. Synthesis of ZSM-5 zeolite from illite mineral. *Microporous Mesoporous Mater.* **2019**, *280*, 324–330. [CrossRef]
17. Wang, J.Q.; Huang, Y.X.; Pan, Y.; Mi, J.X. Synthesis of zeolite A from kaolin by a new method. *Microporous Mesoporous Mater.* **2014**, *199*, 50–56. [CrossRef]
18. Bolshakov, A.; Kosinov, N.; Romero Hidalgo, D.E.; Mezari, B.; van Hoof, A.J.F.; Hensen, E.J.M. Controlled generation of mesopores in ZSM-5 zeolite by treatment with aqueous solutions of NH_4F and NaOH. *Catal. Sci. Technol.* **2019**, *9*, 4239–4247. [CrossRef]
19. Přech, J.; Bozhilov, K.N.; El Fallah, J.; Barrier, N.; Valtchev, V. Top-down synthesis of nanosized FAU-type zeolite. *Microporous Mesoporous Mater.* **2019**, *280*, 297–305. [CrossRef]
20. Si, D.Y.; Zhu, M.H.; Sun, X.M.; Xue, M.; Li, Y.Q.; Wu, T.; Gui, T.; Kumakiri, I.; Chen, X.S.; Kita, H. Formation process and pervaporation of high aluminum ZSM-5 zeolite membrane with fluoride-containing and organic template-free gel. *Sep. Purif. Technol.* **2021**, *257*, 117891. [CrossRef]
21. Meng, X.; Qin, Y.; Zhang, Y.; Li, M.; Huang, H.; Peng, J.; Zhou, L.; Feng, J. The Synergistic Impact of Crystal Seed and Fluoride Ion in the Synthesis of Silicalite-1 Zeolite in Low-Template Systems. *Materials* **2024**, *17*, 266. [CrossRef]
22. Feriancová, A.; Pajtášová, M.; Palliesková, J.; Ondrušová, D.; Kopcová, M.; Jóna, E.; Mojumdar, S.C. Thermal analysis and infrared spectroscopy of kaolin. *J. Therm. Anal. Calorim.* **2013**, *112*, 1047–1052. [CrossRef]
23. Chen, Y.; Zhou, C.; Alshameri, A.; Zhou, S.; Ma, Y.; Sun, T.; Liang, H.; Gong, Y.; Wang, H.; Yan, C. A study on the thermal behavior of kaolinite. *Ceram. Int.* **2014**, *40*, 11751–11758. [CrossRef]
24. Buhl, J.C.; Stemme, F.; Poltz, I. Synthesis and characterization of nitrate containing sodalite. *Microporous Mesoporous Mater.* **2009**, *126*, 276–282. [CrossRef]
25. Malonda Shabani, J.; Babajide, O.; Oyekola, O.; Petrik, L. Synthesis and Characterization of Sodalite Zeolite from South African Coal Fly Ash. *Catalysts* **2019**, *9*, 1033.
26. Cannane, N.O.A.; Rajendran, M.; Selvaraju, R. Synthesis and characterization of silica-alumina mixed oxides. *Spectrochim. Acta A Mol. Biomol. Spectrosc.* **2013**, *110*, 46–54. [CrossRef] [PubMed]
27. Zhang, S.; Zhang, X.; Peng, H.; Wen, L.; Qiu, G.; Hu, M.; Bai, C. Preparation of amorphous silica-alumina from kaolin. *ISIJ Int.* **2014**, *54*, 734–742. [CrossRef]
28. Chen, Z.; Li, Z.; Zhang, Y.; Chevella, D.; Li, G.; Chen, Y.; Guo, X.; Liu, J.; Yu, J. A hierarchical ZSM-5 zeolite with intracrystalline mesopores for the catalytic cracking of n-dodecane. *Chem. Eng. J.* **2020**, *388*, 124322. [CrossRef]
29. Yang, J.; Huang, Y.X.; Pan, Y.; Mi, J.X. Synthesis of ZSM-5 zeolite from kaolin using a two-step crystallization method. *Microporous Mesoporous Mater.* **2020**, *303*, 110247. [CrossRef]
30. Wang, H.; Ma, Z.; Yang, J. Synthesis of hierarchical ZSM-5 zeolite by a dual-template method for the methanol to propylene reaction. *Catal. Lett.* **2020**, *150*, 1454–1461. [CrossRef]
31. Tamizhdurai, P.; Krishnan, P.S.; Ramesh, A.; Shanthi, K. Synthesis and characterization of ZSM-5 catalysts for the conversion of ethanol to hydrocarbons. *Polyhedron* **2018**, *154*, 314–324. [CrossRef]
32. Yaripour, F.; Shariatinia, Z.; Sahebdelfar, S.; Irandoukht, A. Methanol to olefin conversion over nano-ZSM-5 catalysts: Effect of crystal size on catalyst performance. *J. Nat. Gas Sci. Eng.* **2015**, *22*, 260–269. [CrossRef]
33. Yue, Y.; Kang, Y.; Bai, Y.; Gu, L.; Liu, H.; Bao, J.; Wang, T.; Yuan, P.; Zhu, H.; Bai, Z.; et al. Synthesis of hierarchical ZSM-5 zeolite from natural kaolin for catalytic cracking of n-hexane. *Appl. Clay Sci.* **2018**, *158*, 177–185. [CrossRef]
34. Wang, Q.; Xu, S.; Chen, J.; Wei, Y.; Li, J.; Fan, D.; Yu, Z.; Qi, Y.; He, Y.; Xu, S.; Yuan, C.; Zhou, Y.; Wang, J.; Zhang, M.; Su, B.; Liu, Z. Synthesis of hierarchical ZSM-5 zeolites with tunable mesoporosity and acidity for the methanol to propylene reaction. *RSC Adv.* **2014**, *4*, 21479–21491. [CrossRef]
35. Han, S.; Liu, Y.; Yin, C.; Jiang, N. Synthesis of hierarchical ZSM-5 zeolite from diatomite for catalytic cracking of n-heptane. *Microporous Mesoporous Mater.* **2019**, *275*, 223–228. [CrossRef]

36. Wang, J.J.; Tan, Z.C.; Zhu, C.C.; Miao, G.; Kong, L.Z.; Sun, Y.H. Green synthesis of hierarchical ZSM-5 zeolite with tunable acidity for the catalytic conversion of glucose to 5-hydroxymethylfurfural. *Green Chem.* **2016**, *18*, 452–460. [CrossRef]
37. Schmidt, F.; Lohe, M.R.; Büchner, B.; Giordanino, F.; Bonino, F.; Kaskel, S. Hierarchical ZSM-5 zeolites: A comparative study of steaming and desilication. *Microporous Mesoporous Mater.* **2013**, *165*, 148–157. [CrossRef]
38. van Koningsveld, H.; Jansen, J.C.; van Bekkum, H. The monoclinic framework structure of zeolite H-ZSM-5. Comparison with the orthorhombic framework of as-synthesized ZSM-5. *Zeolites* **1990**, *10*, 235–242. [CrossRef]
39. Kashchiev, D. On the Kossel-Stranski Theory of Crystal Growth. *Cryst. Growth Des.* **2012**, *12*, 3257–3262. [CrossRef]

Disclaimer/Publisher's Note: The statements, opinions and data contained in all publications are solely those of the individual author(s) and contributor(s) and not of MDPI and/or the editor(s). MDPI and/or the editor(s) disclaim responsibility for any injury to people or property resulting from any ideas, methods, instructions or products referred to in the content.